Modeling crack growth from pores under compressive loading with application to metallic glasses

Xiaoqing Jin [a,*], Gongyao Wang [b], Leon M. Keer [a], Peter K. Liaw [b], Q. Jane Wang [a]

[a] Department of Mechanical Engineering, Northwestern University, Evanston, IL 60208, USA
[b] Department of Materials Science and Engineering, The University of Tennessee, Knoxville, TN 37996, USA

ARTICLE INFO

ABSTRACT

The mechanism of the fatigue-crack growth is essential to understand the fatigue and fracture behavior of bulk metallic glasses (BMGs) and is thus critical to predict the service lifetime of BMGs as potential engineering structural materials. Experiments indicate that fracture under compressive loading exhibits distinct behaviors different from that under tensile loading. A typical compression failure may initiate from micro porosity where cracks propagate in a direction generally parallel to the loading axis. Micromechanical stress analysis shows that pores cause axial tensile microcracks emanating from the pore. A simplified computational model based on the linear elastic fracture mechanics (LEFM) is proposed to investigate crack initiation and subsequent propagation under compressive load, where the effect of crack closure on mode-I fracture is considered. The stable crack length is characterized by a dimensionless fracture-mechanics quantity required to attain the associated crack length. The behavior of crack growth is examined based on the stress-intensity-factor (SIF) calculation, and its dependence on the loading and lateral confinement conditions is discussed.

© 2011 Elsevier B.V. All rights reserved.

1. Introduction

Bulk metallic glasses (BMGs) [1,2] are regarded as potential new-generation structural materials because of their interesting mechanical properties, such as high hardness and superior strength, good fracture toughness and excellent corrosion resistance. In contrast to the traditional deformation mechanism associated with conventional crystalline materials, the underlying exploration of the mechanical behavior of BMGs is less firmly established. However, there is clear evidence [3–5] that monolithic BMGs usually suffer an inherent drawback in its brittleness and limited ductility, caused by the absence of dislocations and grain boundaries in amorphous alloys. At room temperature, BMGs deform inhomogeneously, where the plastic flow is usually confined in highly localized shear bands. This deformation feature may cause catastrophic failure in service in the form of large strain softening and abrupt rupture and has critically limited the engineering applications of such otherwise highly promising materials.

Mechanisms of fracture and fatigue failure of BMGs are even less well understood [1,6]. Fractures in BMGs have been observed to initiate from casting defects, such as porosities, inclusions, or surface flaws [7,8]. In other studies, fatigue cracks under cyclic loading are reportedly initiated from shear bands, which generally form near flaws, defects, or machining marks in BMGs [4,6]. The formation and propagation of shear bands are usually explained by the free-volume theory [9]. Under a general three-point bending load [8], a fatigue crack initiates from the opened shear band. Then, the fatigue crack will advance at every fatigue cycle in a direction normal to the tensile-stress direction.

To fully exploit the advantageous properties of BMGs for engineering applications, the fracture and fatigue studies are of theoretical as well as practical interest. Experiments indicate that most metallic glasses display the distinct deformation and fracture behavior under compressive loading that differ from those under tensile loading [5,7,10]. When microcracks develop under compression, they do not necessarily lead to sudden failure. As a crack grows to a certain extent, the driving stress-intensity factor may be restrained by the applied compressive-stress field. Consequently, crack growth is arrested, and a variation in the applied stress is required to cause it to grow further. However, this crack-extension behavior is extremely sensitive to the end conditions [11,12]: the lateral constraints due to misalignment, overconstraining the sample ends, and off-axis loading, can all lead to distinct fracture modes.

2. Modeling

In a previous paper [7], the mechanical and fatigue behaviors of the $Ca_{65}Mg_{15}Zn_{20}$ (atomic percent, at. %) BMG were investigated for both monotonic compression loading
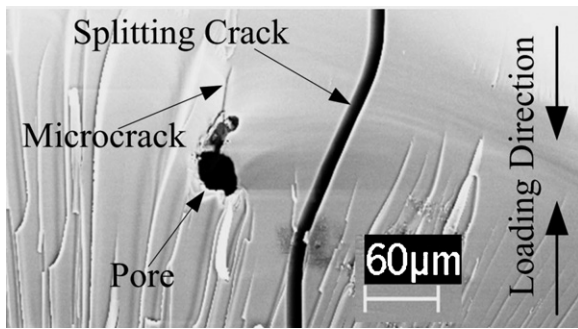
Fig. 1. SEM fractographs indicate a pore-like flaw, microcrack, and splitting crack on the fracture surface of a $Ca_{65}Mg_{15}Zn_{20}$ BMG.

Fig. 3. A contour view of a distribution of the normalized circumferential stress.

and compression–compression fatigue loading. The compression experiments were performed on cubical samples ($4\,mm \times 4\,mm \times 4\,mm$) at room temperature. Spherical voids (typically 25–$50\,\mu m$ in diameter) were observed on the fracture surface. Such micro-flaws as cracks, pores, or weak inclusions functioned as primary crack-nucleation sites (Fig. 1), where a typical microcrack was seen to initiate and propagate a short distance. The preferential sites for crack-nucleation and the initial direction of the crack propagation were in good agreement with the numerical results yielded by finite-element analyses [13]. Moreover, the fracture surface also exhibited a dominant splitting-fracture mode. Under cyclic compression, splitting failure involves a sequence of progressive microfracturing, which may initiate at the pore-like flaws, gradually turning towards the direction of compression (Fig. 1). The final macroscopic splitting failure was critically governed by the fatigue-crack-propagation mechanism [11].

In the present work, we study the crack growth from a circular hole subjected to a far-field compressive stress. The basic geometric configuration of the two-dimensional modeling is depicted schematically in Fig. 2. The origin of the coordinate system is placed at the center of the circular hole of a radius, r_0, in an infinitely extended solid. A crack of length, a, emanates from the perimeter of the circular hole. The orientation angles, θ and ϕ, can be an arbitrary combination. In the special case, $\theta = \phi$, the present modeling degenerates to a radial-crack problem, which has been the
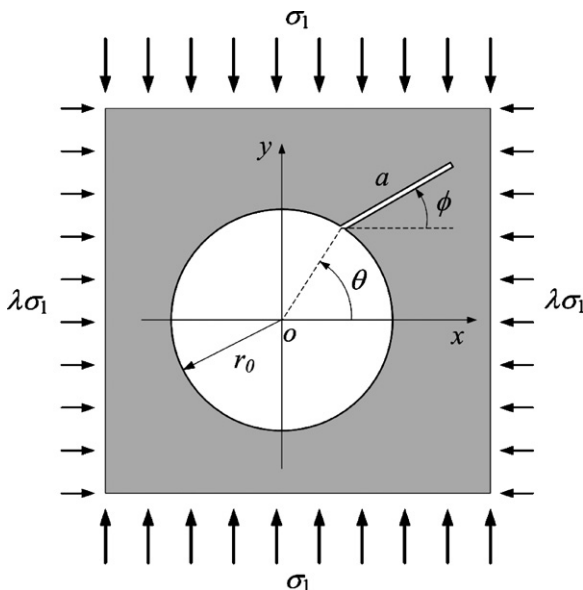
subject of extensive studies [14–16]. The remote compressive load, σ_y, is applied along the y-axis direction. The lateral confinement is simulated by applying a stress, σ_x, along the x-axis direction, where $\sigma_x = \lambda\sigma_y$. For ease of the following presentation, we denote the magnitude of σ_y as σ_1, i.e., $\sigma_1 = |\sigma_y|$, since σ_y is a negative quantity. The confinement is compression for $\lambda > 0$, and tension for $\lambda < 0$, respectively. Note that the special case of $\lambda = 0$ corresponds to the uniaxial compression.

Lin et al. [15] has proposed a versatile and efficient computational method to solve the stress-intensity factor (SIF) of radial cracks emanating from circular holes. Their method of solution [15] is a Green's function based approach [17], where the basic unknowns are the derivative of the crack-opening displacements (COD). This choice of basic unknowns is just one of many options [18], such as crack opening displacement, concentrated force or force doublet on crack faces. For crystalline materials, the derivative of the COD is mathematically analogous to the term dislocation. (As pointed out in [17, p. 191], however, the distinction should be noted between the mathematical dislocation in Continuum Mechanics and the atomic defect dislocation in Material Science.) There is no such correspondence in BMG materials. Nevertheless, the well-established method of solution [15] is still applicable in determining SIFs for BMGs.

For the present problem, the numerical approach of Lin et al. [15] may be extended with the assistance of the appropriate coordinate transformation (cf., Eqs. (2) and (9) in [19]). Note that the method of solution may readily be refined to apply to kinked branches [20] as well as partially closed cracks [14]. It is also worth pointing out that the effect of crack closure on mode-I SIF must be taken into account for fracture under compression, which is less well documented (see e.g., the handbook [16]). To address this problem, it is necessary to examine the stress field around the circular hole in the absence of the crack: the circumferential stress under uniaxial compression ($\lambda = 0$) is given by [21]:

$$\frac{\sigma_\theta(r, \theta)}{\sigma_1} = -\frac{1}{2}\left[1 + \frac{r_0^2}{r^2} + \left(1 + 3\frac{r_0^4}{r^4}\right)\cos 2\theta\right] \tag{1}$$

In view of symmetry, the right-hand side Eq. (1) in the first quadrant is plotted in contour view (Fig. 3). It is seen that the maximum tensile stress occurs at the north pole ($r = r_0$, $\theta = 90°$), which is expected to cause tensile microcracks, as evidenced in Fig. 1. The tensile circumferential stresses fall rapidly within a small region for $\theta > 60°$ and a radial distance, $r < \sqrt{3}r_0$. One may expect that a

Fig. 2. A two-dimensional linear-elastic fracture-mechanics based modeling.
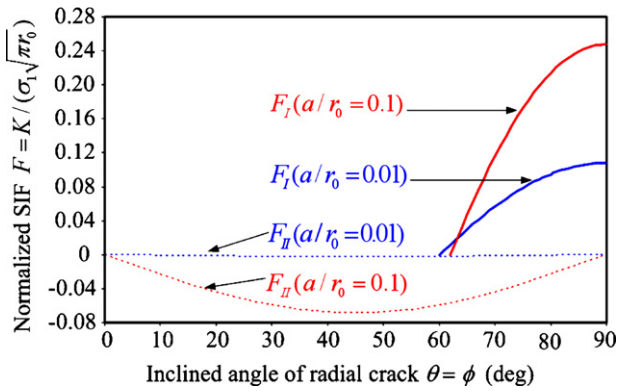
Fig. 4. SIF results of short radial cracks emanating from a circular hole.

crack developing outside this tensile zone could be fully or partially closed.

3. Results and discussion

The stress distribution (Fig. 3) indicates that crack closure is a salient feature of fracture under compressive loading. This effect is carefully taken into account in the present computation. However, the crack-face friction is ignored for simplicity. In the following discussion, the mode-I and mode-II SIFs, i.e., K_I and K_{II}, respectively, are normalized by a factor, $\sigma_1\sqrt{\pi r_0}$:

$$K_I = \sigma_1\sqrt{\pi r_0}F_I, \qquad K_{II} = \sigma_1\sqrt{\pi r_0}F_{II} \qquad (2)$$

where the non-dimensionalized SIFs [16], F_I and F_{II}, are functions of λ, a/r_0, θ, and ϕ.

Consider first a radial crack emanating from a circular hole subjected to uniaxial compression. Computations on two short cracks ($a/r_0 = 0.01$ or 0.1) are performed to investigate the properties of crack initiation. Fig. 4 shows the variation of F_I and F_{II} for different inclined angles, θ. For both cases, it is seen the mode-I SIF vanishes for θ smaller than $60°$, since the crack faces are closed. A maximum F_I occurs at $\theta = 90°$, in which case a pure mode I is evidenced due to symmetry. For the shorter crack ($a/r_0 = 0.01$), the mode-II SIF tends to be orders of magnitude smaller. This trend demonstrates that a radial crack is much easier to be initiated by the mode-I splitting instead of the mode II shearing. However, for a pre-existing crack whose length is comparable to one tenth of the radius of the circular hole, the mode-II effect may not be negligible, and it becomes paramount when crack closure is involved (cf., $0° < \theta < 60°$ in Fig. 4).

At the north pole ($\theta = 90°$) of the circular hole, the mode-I SIF calculation is performed for different crack orientation angles, ϕ. The closure of a crack ($a/r_0 = 0.1$) is observed for $\phi < 58°$, and a variation of F_I is shown in Fig. 5. The maximum of F_I is attained for a
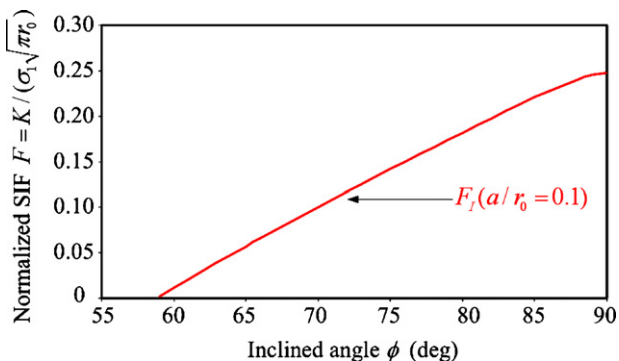

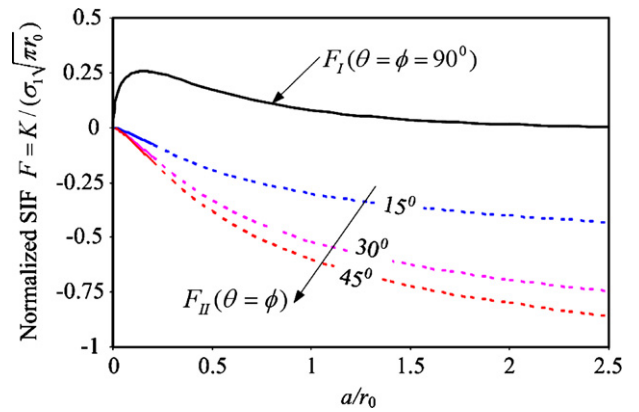**Fig. 5.** Effect of crack closure on a crack originated at the north pole of the hole.

Fig. 6. Variation of SIF vs. the length of a radial crack emanating from a circular hole.

vertical splitting crack ($\phi = 90°$). The present analysis suggests that the microcrack under global compressive loading may be produced by a local tensile stress. The modeling results predict that when the BMG is subjected to uniaxial compression, a crack may nucleate at the north pole of the cavity and propagate in a direction parallel to the loading axis, which are in excellent agreement with the experimental observation of the microcrack in Fig. 1.

To study the behavior of crack propagation, numerical computations are performed for radial cracks with an increasing length (Fig. 6). The crack length under consideration is $0 < a/r_0 < 2.5$. Only mode-II SIFs are plotted for $\theta = 15°$, $30°$, and $45°$, since in these cases a crack is fully closed. It is seen that F_{II} tends to increase as the crack becomes longer, while $\theta = 45°$ yields the greatest F_{II}. However, the variation of F_I for $\theta = \phi = 90°$ exhibits an interesting transition: the mode-I SIF first increases and attains its maximum at $a/r_0 = 0.16$, then gradually decreases afterwards. The crack tip is closed, and F_I drops to zero at $a/r_0 = 2.65$. This trend expects that the mode-I crack-driving force will decrease after a crack propagates to a certain distance. Therefore, under uniaxial compression, the vertical splitting microcrack will ultimately be fully arrested, as evidenced in the experiment (Fig. 1).

According to the fracture-mechanics theory, the crack grows until the SIF equals to the fracture toughness, K_c. This condition corresponding to mode-I cracking at $\theta = \phi = 90°$ is

$$K_I = K_{IC} \qquad (3)$$

Substituting the first of Eq. (2) into Eq. (3), we may define a dimensionless compressive load, p^*, shown below:

$$p^* = \frac{\sigma_1\sqrt{\pi r_0}}{K_{IC}} = \frac{1}{F_1} \qquad (4)$$

Physically, p^* corresponds to the magnitude of the compressive loading, σ_1, required to attain the associated crack configuration [11]. From Fig. 6, it is expected that p^* for $\theta = \phi = 90°$ will first decrease (till $a/r_0 = 0.16$), and then increase to infinity. In other words, an unstable crack growth is experienced during crack initiation, and when the crack develops to a certain distance ($a/r_0 = 0.16$), it continues to grow in a stable manner, requiring an increase in the applied load for each increment of crack growth.

Finally, the effect of lateral confinement is considered. The results of the dimensionless quantity, p^*, are plotted for various values of λ (Fig. 7), which may then be used to interpret the stability of crack growth. Although in all the cases, the crack growth is unstable, when the crack length is small ($a/r_0 \sim 0.1$), the subsequent crack-propagation behavior is seen to be extremely sensitive to λ. The crack growth tends to be stable for all values of $\lambda \geq 0$. However, when the lateral confinement is tensile, e.g., even λ being slightly less than zero, the cracks grow stably at first but ultimately will
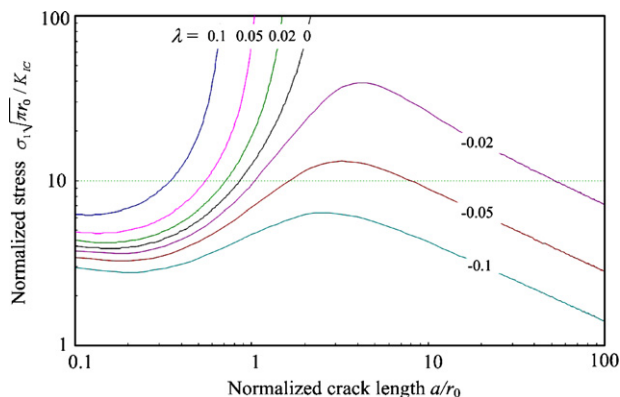
Fig. 7. Effect of lateral confinement on the stability of crack extension.

grow in an unstable fashion. The loading and geometric conditions required to induce unstable growth are significantly influenced by the magnitude of the lateral tension. Moreover, the unstable growth will eventually cause the crack to propagate without limit, leading to global splitting failure, as witnessed in Fig. 1.

The present study may provide helpful guidelines for designing and performing future BMGs fatigue experiments under compression–compression loading. Particularly, a slight end condition change caused by misalignment or over-constraining the samples may cause large systematic errors, since this arrangement may effectively introduce the lateral confinement stress to a certain degree.

4. Conclusions

Compression failure in BMGs tends to be a complex process. The objective of this study is to provide a linear-elastic-fracture-mechanics (LEFM) model to investigate the crack-growth behavior of BMGs under compression loading. The present analysis demonstrates that tensile microcracks may be generated from the pores under a compressive load. The preferential crack-nucleation sites are in good agreement with the experiments. Computation of SIFs for short radial cracks emanating from a circular hole shows that K_{II} is relatively smaller than K_I, which therefore verifies a mode-I dominant theory for fatigue-crack initiation from pores. After the initiation of a microcrack, crack-growth properties are examined from the variation of SIFs with respect to the increasing length. During the crack-growth stage when the crack is partially or fully closed, the numerical results indicate that the mode-II effect becomes significant. The stability of crack extension is studied by a dimensionless quantity, which represents the required magnitude of compressive loads to attain the associated crack length. The analysis results show that the behavior of the crack growth is extremely sensitive to the effect of lateral confinement. Axial splitting can be caused by the unstable growth of macroscopic cracks, resulting from such lateral-confinement effects as misalignment, off-axis loading, or over-constraining the sample ends.

References

[1] C.A. Schuh, T.C. Hufnagel, U. Ramamurty, Acta Materialia 55 (12) (2007) 4067–4109.
[2] W.H. Wang, C. Dong, C.H. Shek, Materials Science and Engineering: R: Reports 44 (2–3) (2004) 45–89.
[3] G.Y. Wang, P.K. Liaw, M.L. Morrison, Intermetallics 17 (8) (2009) 579–590.
[4] G.Y. Wang, P.K. Liaw, A. Peker, B. Yang, M.L. Benson, W. Yuan, W.H. Peter, L. Huang, A. Freels, R.A. Buchanan, C.T. Liu, C.R. Brooks, Intermetallics 13 (3-4) (2005) 429–435.
[5] Z.F. Zhang, J. Eckert, L. Schultz, Acta Materialia 51 (4) (2003) 1167–1179.
[6] C.J. Gilbert, V. Schroeder, R.O. Ritchie, Metallurgical and Materials Transactions A – Physical Metallurgy and Materials Science 30 (7) (1999) 1739–1753.
[7] G. Wang, P.K. Liaw, O.N. Senkov, D.B. Miracle, M.L. Morrison, Advanced Engineering Materials 11 (1-2) (2009) 27–34.
[8] G. Wang, P.K. Liaw, X. Jin, Y. Yokoyama, E.W. Huang, F. Jiang, L.M. Keer, A. Inoue, Journal of Applied Physics 108 (11) (2010) 113512.
[9] A.S. Argon, Acta Metallurgica 27 (1) (1979) 47–58.
[10] G.Y. Wang, D.C. Qiao, Y. Yokoyama, M. Freels, A. Inoue, P.K. Liaw, Journal of Alloys and Compounds 483 (1-2) (2009) 143–145.
[11] S. Nemat-Nasser, H. Horii, Journal of Geophysical Research 87 (Nb8) (1982) 6805–6821.
[12] C.G Sammis, M.F. Ashby, Acta Metallurgica 34 (3) (1986) 511–526.
[13] J. Raphael, G.Y. Wang, P.K. Liaw, O.N. Senkov, D.B. Miracle, Metallurgical and Materials Transactions A – Physical Metallurgy and Materials Science 41A (7) (2010) 1775–1779.
[14] M. Comninou, F.K. Chang, International Journal of Fracture 28 (1) (1985) 29–36.
[15] S. Lin, D.A. Hills, D. Nowell, Journal of Strain Analysis 31 (3) (1996) 235–242.
[16] Y. Murakami, Stress Intensity Factors Handbook, Pergamon, Oxford, 1986.
[17] J.R. Barber, Elasticity, Kluwer Academic Publishers, Dordrecht, 2004.
[18] Y.Z. Chen, Engineering Fracture Mechanics 51 (1) (1995) 97–134.
[19] X. Jin, L.M. Keer, International Journal of Fracture 137 (1–4) (2006) 121–137.
[20] X. Jin, L.M. Keer, E.L. Chez, International Journal of Fracture 142 (3–4) (2007) 219–232.
[21] S. Timoshenko, J.N. Goodier, Theory of Elasticity, McGraw-Hill, New York, 1987.